J|A|C|S ARTICLES

Published on Web 03/17/2010

De Novo Designed Coiled-Coil Proteins with Variable Conformations as Components of Molecular Electronic Devices

Clara Shlizerman,[†,||] Alexander Atanassov,[‡,||] Inbal Berkovich,[†] Gonen Ashkenasy,*[,†] and Nurit Ashkenasy*[,‡,§]

Department of Chemistry, Department of Materials Engineering, and Ilse Katz Institute for Nanoscale Science and Technology, Ben Gurion University of the Negev, Beer Sheva, Israel

Received September 17, 2009; E-mail: gonenash@bgu.ac.il; nurita@bgu.ac.il

Abstract: Conformational changes of proteins are widely used in nature for controlling cellular functions, including ligand binding, oligomerization, and catalysis. Despite the fact that different proteins and artificial peptides have been utilized as electron-transfer mediators in electronic devices, the unique propensity of proteins to switch between different conformations has not been used as a mechanism to control device properties and performance. Toward this aim, we have designed and prepared new dimeric coiled-coil proteins that adopt different conformations due to parallel or antiparallel relative orientations of their monomers. We show here that controlling the conformation of these proteins attached as monolayers to gold, which dictates the direction and magnitude of the molecular dipole relative to the surface, results in quantitative modulation of the gold work function. Furthermore, charge transport through the proteins as molecular bridges is controlled by the different protein conformations, producing either rectifying or ohmic-like behavior.

Introduction

The unique primary sequences of proteins dictate their secondary and tertiary structures that give rise to their specific activities.[1] Understanding the parameters that govern protein folding and protein−protein interactions makes it possible to design artificial peptides and proteins with excellent control over their secondary structures and in some cases also over super-secondary and tertiary structures. Protein motions, and specifically major conformational changes, complement the static three-dimensional structures of proteins and allow them to bind ligands, form oligomers, aggregate, and perform mechanical work and catalytic activity. The ability to control conformational changes may thus enable quantitative manipulation of artificial protein functions, but this challenge is rarely met.[2−4] As part of our program to incorporate functional peptide and protein scaffolds into electronic devices,[5−11] we test here the possibility to control the surface electronic properties of conducting materials and the performance of molecular devices using de novo designed coiled-coil proteins that adopt significantly different conformations.

α-Helical coiled-coil structures are found in about 5% of all native proteins, where they serve as oligomerization domains affecting the quaternary structures and association dynamics. Due to their high regularity and relative simplicity, they appear to be primary candidates for the design of functional molecules.[12−20] Thus, artificial coiled-coil systems have been constructed during the past few years, and their solvent-exposed surfaces, and in some cases also the buried hydrophobic cores, were exploited for different purposes in solution, such as catalysis, sensing, binding to protein recognition domains, and energy and electron transfer. Furthermore, the design of coiled-

[||] These authors contributed equally.
[†] Department of Chemistry.
[‡] Department of Materials Engineering.
[§] Ilse Katz Institute for Nanoscale Science and Technology.

(1) Gerstein, M.; Echols, N. *Curr. Opin. Chem. Biol.* **2004**, *8*, 14–19.
(2) Woolley, G. A. *Acc. Chem. Res.* **2005**, *38*, 486–493.
(3) Saucede, L.; Dos Santos, S.; Chandravarkar, A.; Mandal, B.; Mimna, R.; Murat, K.; Camus, M.-S.; Berard, J.; Grouzmann, E.; Adrian, M.; Dubochet, J.; Lopez, J.; Lashuel, H.; Tuchscherer, G.; Mutter, M. *Chimia* **2006**, *60*, 199–202.
(4) Mohammed, J. S.; Murphy, W. L. *Adv. Mater.* **2009**, *21*, 2361–2374.
(5) Ashkenasy, G.; Cahen, D.; Cohen, R.; Shanzer, A.; Vilan, A. *Acc. Chem. Res.* **2002**, *35*, 121–128.
(6) Ashkenasy, G.; Ghadiri, M. R. *J. Am. Chem. Soc.* **2004**, *126*, 11140–11141.
(7) Ashkenasy, N.; Sanchez-Quesada, J.; Bayley, H.; Ghadiri, M. R. *Angew. Chem., Int. Ed.* **2005**, *44*, 1401–1404.
(8) Horne, W. S.; Ashkenasy, N.; Ghadiri, M. R. *Chem.—Eur. J.* **2005**, *11*, 1137–1144.
(9) Ashkenasy, N.; Horne, W. S.; Ghadiri, M. R. *Small* **2006**, *2*, 99–102.
(10) Wagner, N.; Ashkenasy, G. *Chem.—Eur. J.* **2009**, *15*, 1765–1775.
(11) Yemini, M.; Hadad, B.; Liebes, Y.; Goldner, A.; Ashkenasy, N. *Nanotechnology* **2009**, *20*, 245302/1–245302/6.
(12) Oakley, M. G.; Hollenbeck, J. J. *Curr. Opin. Struct. Biol.* **2001**, *11*, 450–7.
(13) Baltzer, L.; Nilsson, J. *Curr. Opin. Biotech.* **2001**, *12*, 355–360.
(14) Jarvo, E. R.; Miller, S. J. *Tetrahedron* **2002**, *58*, 2481–2495.
(15) Kritzer, J. A.; Stephens, O. M.; Guarracino, D. A.; Reznik, S. K.; Schepartz, A. *Bioorg. Med. Chem.* **2004**, *13*, 11–16.
(16) Schnarr, N. A.; Kennan, A. J. *J. Am. Chem. Soc.* **2004**, *126*, 14447–14451.
(17) Ghosh, I.; Chmielewski, J. *Curr. Opin. Chem. Biol.* **2004**, *8*, 640–644.
(18) Yadav, M. K.; Leman, L. J.; Price, D. J.; Brooks, C. L., III; Stout, C. D.; Ghadiri, M. R. *Biochemistry* **2006**, *45*, 4463–4473.
(19) Hadley, E. B.; Gellman, S. H. *J. Am. Chem. Soc.* **2006**, *128*, 16444–16445.
(20) Hadley, E. B.; Testa, O. D.; Woolson, D. N.; Gellman, S. H. *Proc. Natl. Acad. Sci. U.S.A.* **2008**, *105*, 530–535.

 10.1021/ja907902h

coil proteins that can undergo conformational changes in solution was exploited in order to achieve dynamic control over their functionality.[2,3,6,21−23] Examples include the design of conformational switches affecting DNA binding properties and dimer to trimer equilibrations that resulted in changes in catalytic behavior.

Redox active proteins and protein domains from the natural photosystems were previously explored as electron-transfer mediators in molecular junctions.[24−28] Several synthetic systems that comprise α-helical peptides,[29−34] amyloids,[35] and peptide nanotubes[8,9] were utilized in a complementary approach, in order to study the relations between structural parameters and charge-transfer characteristics. It was shown that the intrinsic molecular dipole of α-helical systems affects the work function of gold, which can thus be modulated by the relative orientation and length of the peptide.[33,36] When the mechanisms of charge transfer through such helical peptides in molecular junctions were studied, it was suggested that the internal dipole of the molecules induces rectifying behavior of the current−voltage curve.[30,37,38] Voltage-induced switching of molecular junction conductance was demonstrated recently using helical peptides and explained by a small conformational change, from α-helix to 3_{10} helix, following the interaction of the applied electric field with the large dipole moment of the helix.[39] However, the tendency of proteins to switch between significantly different conformations, which as mentioned above is a principle tool for controlling their functionality in nature, has been generally overlooked. In this work, we describe the utilization of different conformations of de novo designed heterodimeric coiled-coil proteins as means to control their functions in molecular electronic applications. Toward this aim, we show that proteins that are very similar in primary sequence but adopt different conformations due to parallel or antiparallel relative orientation of their monomers can be utilized to manipulate incrementally the work function of conductive surfaces and furthermore to affect charge-transfer processes in molecular junction configurations.

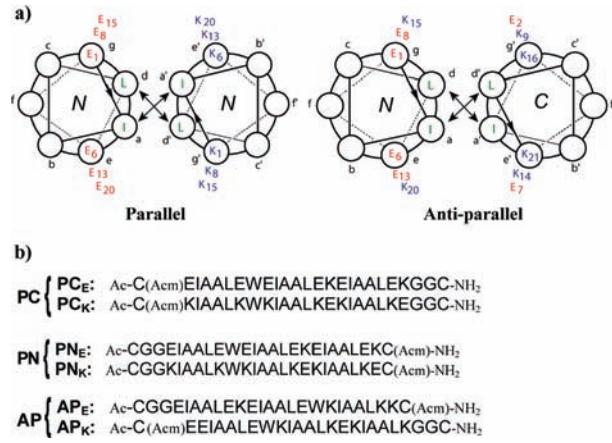

Figure 1. (a) Helical wheel presentations of parallel and antiparallel coiled-coil structures, showing the seven amino acid repeats. The Ile-Leu hydrophobic core is highlighted in green, and the Lys-Glu charge matching between *e* and *g* positions that flank the hydrophobic core on the opposing helices is shown in blue and red. Predefined mutations at the *e* and *g* positions facilitated the formation of the non-native antiparallel structure. (b) Primary sequences of peptides that compose the parallel (**PC**), with free Cys thiols at the C-terminal, (**PN**), with free Cys thiols at the N-terminal, and antiparallel (**AP**) coiled coils. **PN**, which is composed of the same monomer sequences of **PC** that form a parallel structure, is expected to be oriented in an opposite direction relative to **PC**, namely with the N-termini thiols attached to gold (see explanation in the text). The subscript E denotes glutamic acid rich peptides and the subscript K the opposing lysine rich peptides.

Results and Discussion

Design, Synthesis, And Solution Characterizations of the Coiled Coils. We have designed, synthesized, and characterized the structure and function of parallel and antiparallel heterodimeric α-helical coiled-coil proteins shown in Figure 1. In this system, the different protein conformations are expected to affect differently the properties of gold surfaces and the performance of the proteins in molecular junction configuration due to changes in the monomers' relative orientation with respect to each other, which implies a significantly different net molecular dipole of the dimeric structures. A substantial dipole going from the C- to N-terminus is present in the parallel structure, while the antiparallel structure possesses a much smaller dipole because the dipole of one monomer is canceled out by the other upon dimerization. The design of the three protein analogues was based on the principles that guided the formation of the "Velcro" coiled coils, which provide optimal charge matching between the interfaces of one helix and the other.[12,40,41] Since short molecules are expected to be more efficient bridges in molecular junctions, the actual sequences were based on a shorter "Velcro" motif that is made of 21 amino acid peptides, which form helical structures ∼4.5 nm in length along the main axis,[42] similar in size to other proteins studied as bridges in molecular junctions.[24,28,43] Peptide sequences that follow closely the original "Velcro" structure were used, and

(21) Gross, M. *Curr. Protein Pept. Sci.* **2000**, *1*, 339–47.
(22) Renner, C.; Moroder, L. *ChemBioChem* **2006**, *7*, 868–78.
(23) Pagel, K.; Koksch, B. *Curr. Opin. Chem. Biol.* **2008**, *12*, 730–9.
(24) Davis, J. J.; Morgan, D. A.; Wrathmell, C. L.; Axford, D. N.; Zhao, J.; Wang, N. *J. Mater. Chem.* **2005**, *15*, 2160–2174.
(25) Willner, B.; Katz, E.; Willner, I. *Curr. Opin. Biotechnol.* **2006**, *17*, 589–596.
(26) Schlag, E. W.; Sheu, S. Y.; Yang, D. Y.; Selzle, H. L.; Lin, S. H. *Angew. Chem., Int. Ed.* **2007**, *46*, 3196–3210.
(27) Davidson, V. L. *Acc. Chem. Res.* **2008**, *41*, 730–738.
(28) Jin, Y. D.; Honig, T.; Ron, I.; Friedman, N.; Sheves, M.; Cahen, D. *Chem. Soc. Rev.* **2008**, *37*, 2422–2432.
(29) Yasutomi, S.; Morita, T.; Imanishi, Y.; Kimura, S. *Science* **2004**, *304*, 1944–1947.
(30) Sek, S.; Swiatek, K.; Misicka, A. *J. Phys. Chem. B* **2005**, *109*, 23121–23124.
(31) Sek, S.; Misicka, A.; Swiatek, K.; Misicka, E. *J. Phys. Chem. B* **2006**, *110*, 19671–19677.
(32) Takeda, K.; Morita, T.; Kimura, S. *J. Phys. Chem. B* **2008**, *112*, 12840–12850.
(33) Kimura, S. *Org. Biomol. Chem.* **2008**, *6*, 1143–1148.
(34) Okamoto, S.; Morita, T.; Kimura, S. *Langmuir* **2009**, *25*, 3297–3304.
(35) del Mercato, L. L.; Pompa, P. P.; Maruccio, G.; Della Torre, A.; Sabella, S.; Tamburro, A. M.; Cingolani, R.; Rinaldi, R. *Proc. Natl. Acad. Sci. U.S.A.* **2007**, *104*, 18019–18024.
(36) Miura, Y.; Kimura, S.; Kobayashi, S.; Iwamoto, M.; Imanishi, Y.; Umemura, J. *Chem. Phys. Lett.* **1999**, *315*, 1–6.
(37) Kitagawa, K.; Morita, T.; Kimura, S. *Langmuir* **2005**, *21*, 10624–10631.
(38) Kitagawa, K.; Morita, T.; Kimura, S. *Thin Solid Films* **2006**, *509*, 18–26.
(39) Kitagawa, K.; Morita, T.; Kimura, S. *Angew. Chem., Int. Ed.* **2005**, *44*, 6330–6333.
(40) O'Shea, E. K.; Lumb, K. J.; Kim, P. S. *Curr. Biol.* **1993**, *3*, 658–67.
(41) Kim, B.-M.; Oakley, M. G. *J. Am. Chem. Soc.* **2002**, *124*, 8237–8244.
(42) De Crescenzo, G.; Litowski, J. R.; Hodges, R. S.; O'Connor-McCourt, M. D. *Biochemistry* **2003**, *42*, 1754–1763.
(43) Maruccio, G.; Marzo, P.; Krahne, R.; Passaseo, A.; Cingolani, R.; Rinaldi, R. *Small* **2007**, *3*, 1184–1188.

their dimers were expected to form a parallel structure. The peptides were additionally equipped with cysteine residues as gold anchoring units on both ends, with a Cys thiol on one end of each peptide blocked by an Acm group to enable self-assembly of the coiled-coil proteins in a predefined unidirectional manner with the molecular dipole pointing out (**PC**) or into (**PN**) the surface. It is well established that the folding, partner specificity, and oligomerization state of coiled coils are all influenced by interactions that occur among the *a*, *d*, *e*, and *g* heptad positions of opposing helices (Figure 1a).[19,20,44−46] Thus, the design of **AP** to form the antiparallel structure was achieved by mutating amino acids at the charged *e* and *g* positions of the parallel structure forming peptides. These changes excluded the formation of parallel structures via negative design, calculated to be in the order of 5 kcal/mol,[47] while gaining perfect charge matching in the antiparallel conformation (Figure 1a).

All monomeric peptides were synthesized by solid-phase Fmoc-based synthesis, purified by preparative high-performance liquid chromatography (HPLC), and their molecular weight and purity were characterized by mass spectra and analytical HPLC. It should be noted that apart from mutations at specific *e* and *g* positions as described above, the proteins are practically identical in sequence, a fact that is also reflected by their identical molecular weights (2775 g/mol). The heterodimeric coiled-coil assemblies were formed by equilibrating equimolar solutions of the respective monomers in phosphate buffer at pH = 7.2, in oxidizing environment (air) for at least 30 min. Formation of unique disulfide dimeric structures was monitored by HPLC (Figure 2a,b) and circular dichroism (CD) of 200−500 μM peptide solutions (Figure 2c). For example, a principle single peak at 11.7 min is observed in the HPLC chromatogram of the preformed **AP** dimer, allowing us to infer that most of the monomers assembled into a single coiled-coil structure in the designed orientation to allow disulfide formation (Figure 2a). The addition of a reducing agent (TCEP) to the coiled-coil solution, and consequently disassembly of the disulfide bonds, resulted in the appearance of two peaks in the HPLC chromatogram, at retention times suited for solutions of each of the isolated monomers (Figure 2b). The same procedure has been performed to follow heterodimer formation for **PC** complexes. The CD spectra of all peptides showed molar ellipticity minima at ~208 and 222 nm (Figure 2c). Comparison of the relative intensities of these two minima obtained for solution of the monomers and their corresponding mixtures shows that much deeper minima at ~222 nm were obtained for the mixtures, revealing the clear signature of coiled-coil assembly formation.[48] CD measurements of **AP** under reducing conditions (gray trace) also showed the expected spectrum for coiled-coil structure albeit with somewhat lower molar ellipticity, reflecting the fact that the disulfide bonds provide additional structure stabilization.

Effects of Coiled-Coil Conformations on the Electronic Surface Properties of Gold. In order to study the effects of the new proteins on surface electronic properties, and their performance as molecular bridges, the proteins were self-assembled by immersing freshly prepared gold surfaces in 500 μM solutions of preformed coiled coils in phosphate buffer overnight (Figure 3a). The surface coverage due to adsorption of **PC**, **AP**, and **PN** was estimated from quantitative HPLC measurements of samples obtained by removal of the entire layer using excess amounts of small-molecule thiol (β-mercapto ethanol). The calculated area per molecule for each of the proteins was found to be about 200 A^2 (Figure 3a), correlating well with the previously reported diameter of monomeric α-helix structures (0.9−1.5 nm),[32] thus reflecting high surface coverage for all cases. Ellipsometry measurements indicated the formation of ~4 nm thick layers for the different structures (Figure 3a). In addition, topography imaging by atomic force microscopy (AFM) of squares "shaved" in these monolayers indicated actual thicknesses of 3.8 ± 0.2 nm. By taking into account complete coverage, these measurements suggest the formation of monolayers tilted with an angle of 25−30° with respect to the surface normal. The ability to retain the coiled-coil structures even after adsorption on the gold surfaces was inferred by measuring the

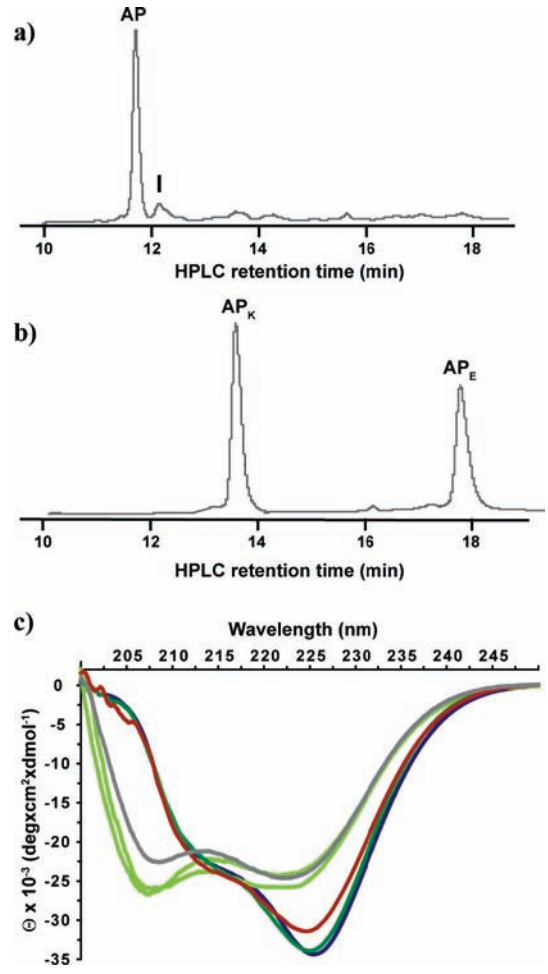

Figure 2. Analysis of coiled-coil dimer formation. (a) HPLC trace obtained after mixing equimolar amounts (500 μM) of the **AP** forming monomers in ambient atmosphere for 30 min (I = minor impurity, tentatively assigned as the $\mathbf{AP_K}$ dimer). (b) HPLC trace obtained after rereducing the pure **AP** dimer to its monomers, using the reducing agent tris(2-carboxyethyl)phosphine hydrochloride (TCEP) for 30 min. Similar results were obtained for dimerization of **PC** from $\mathbf{PC_E}$ and $\mathbf{PC_K}$ (data not shown). (c) CD spectra obtained for 500 μM solutions of **PC** (red), **PN** (blue), and **AP** (green) in phosphate buffer at pH 7.2. The CD spectra obtained for solution of each of the **AP** forming monomers ($\mathbf{AP_E}$ and $\mathbf{AP_K}$) are shown for comparison (light green). The deeper minima at ~222 nm obtained for the dimers is a clear signature of the coiled-coil formation. CD measurements of **AP** under reducing conditions (TCEP) are shown in gray.

(44) Harbury, P. B.; Zhang, T.; Kim, P. S.; Alber, T. *Science* **1993**, *262*, 1401–1407.
(45) Kohn, W. D.; Hodges, R. S. *Trends Biotechnol.* **1998**, *16*, 379–389.
(46) Kohn, W. D.; Kay, C. M.; Hodges, R. S. *J. Mol. Biol.* **1998**, *283*, 993–1012.
(47) Krylov, D.; Barchi, J.; Vinson, C. *J. Mol. Biol.* **1998**, *279*, 959–972.
(48) Sreerama, N.; Woody, R. W. *Circular Dichroism (2nd Ed.)* **2000**, 601–620.

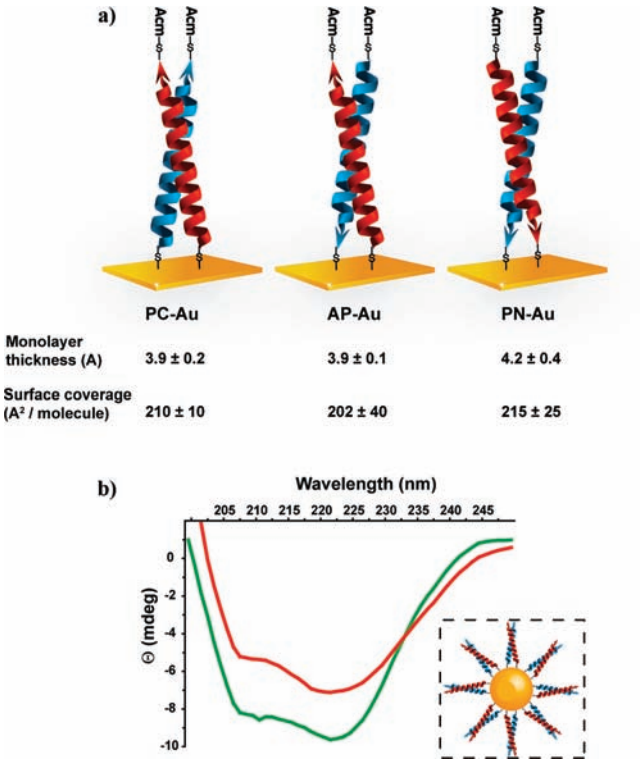

Figure 3. Characterization of protein−gold hybrid structures. (a) Illustration of the parallel and antiparallel coiled coils adsorbed onto gold surfaces. Red is used for glutamic acid rich peptides and blue for lysine rich peptides. **PN-Au** is the hybrid structure obtained after adsorbing a monolayer of a parallel coiled-coil protein with the N-termini thiols attached to the gold (see text). The illustrative arrowheads mark the monomeric molecular dipoles, emphasizing that net molecular dipoles of opposite directions relative to the gold surface are present in the parallel dimeric structures (**PC** vs **PN**), while a negligible dipole is present in the anti parallel structure, **AP**. Monolayer thicknesses measured by ellipsometry, and surface coverage, shown as area per molecule (evaluated by removal of the layers using β-mercapto ethanol), are shown below each of the hybrid structures. (b) CD spectra of **PC** (red) and **AP** (green) adsorbed onto 5 nm gold colloids (0.2 μM) in phosphate buffer at pH 7.2. Each gold colloid was covered by approximately 80 protein molecules; thus, the measurements correspond to a concentration of ~13 μM proteins. The similarity to the spectra obtained for the coiled coils in solution (Figure 2c) provided evidence for retaining the coiled-coil structure during and after the adsorption process.

CD spectra of **PC** and **AP** proteins assembled on 5 nm gold colloids. The appearance of the characteristic minima at 208 and 222 nm (Figure 3b) supported the preservation of the supersecondary structure.

As a result of the significantly different orientations of the peptide monomers with respect to each other in the parallel and antiparallel proteins, a large difference in the molecular dipole is obtained (Figures 3a and 4). This difference can be used to modulate the surface work function of gold to which a monolayer of the protein is attached, which in turn would affect the electronic behavior of a device containing such an interface.[49] By measuring the contact potential difference (CPD) of the gold-monolayer hybrids with respect to a gold reference electrode using the Kelvin probe arrangement (Figure 4), we have found that the gold substrate work function is heavily influenced by the conformation of the coiled-coil structure. The −350 mV CPD measured for **PC-Au**, in which **PC** is attached to gold surface through the C-termini of the peptide monomers, correlates well with the molecular dipole direction pointing away

(49) Vilan, A.; Shanzer, A.; Cahen, D. *Nature* **2000**, *404*, 166–168.

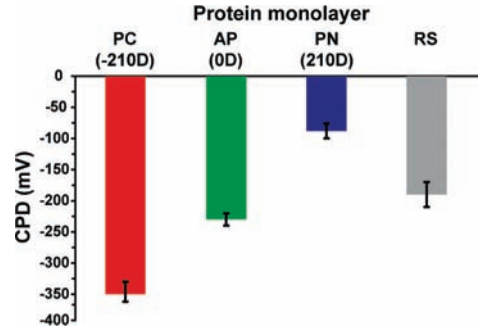

Figure 4. CPD of the coiled-coil gold hybrids. The estimated molecular dipole of each structure is shown in parentheses, calculated using *e*/2 charge for each peptide monomer dipole. The dipole is designated positive when pointing toward the surface. A linear dependence is obtained between the molecular dipole and the CPD of the different molecules. The CPD induced by **RS**, a reference Cys-Gly-Gly-dodecane thiol molecule, shows the effect of the gold−thiol bond.

from the surface as indicated in Figure 3a, thus decreasing the sample work function. The magnitude of the signal is similar to the one obtained with monolayers of helical peptides having a similar number of amino acids,[36] suggesting that similar depolarization effects occur in both systems despite the close proximity of the two helices in the coiled-coil structure. In addition to exploiting the orientation and length of the α-helix peptides to control the work function of gold,[36] the utility of coiled-coil structures enabled increasing the CPD by 130 mV by changing the protein conformation from parallel (**PC-Au**) to antiparallel (**AP-Au**). Due to the absence of protein-induced surface dipole in **AP-Au**, the work function increases toward the reference gold electrode work function. The overall CPD of about −200 mV with respect to the gold reference electrode that was observed for **AP-Au** is due to the polar nature of the gold−thiol bond.[36] This was supported by measuring the CPD of gold surfaces covered with monolayer of **RS**, a reference molecule that consists of a dodecane alkyl chain attached to the short Cys-Gly-Gly tail of the peptide monomers. The CPD value of **RS-Au** and **AP-Au** were found to be identical within experimental errors (Figure 4). To further test if the CPD change can be linearly correlated with changes in the molecular dipole, we have measured the CPD of **PN-Au**, the hybrid structure obtained after adsorbing a monolayer of parallel coiled-coil structures on gold with the molecules oriented in an opposite direction relative to **PC**, namely with the N-termini thiols attached to the gold. As anticipated, the highest CPD value was obtained for **PN-Au**, since the molecular dipole pointing into the surface, inducing an increase in work function. Indeed, we observed a very similar increase in CPD (142 mV) from **AP-Au** to **PN-Au** as from **PC-Au** to **AP-Au**. This linear dependence suggests a direct influence of the coiled-coil net dipole on the gold work function (Figure 4).

We have further combined the ability to modulate the gold surfaces work function by the coiled-coil proteins with a microcontact printing (μCP) technique in order to achieve lateral control of the work function. We have formed line patterns, 5 μm wide with 10 μm period, of each of the proteins on gold surfaces. Kelvin probe force microscopy (KPFM) measurements were used to monitor the lateral variations in the CPD with high resolution (Figure 5a−c). The differences in work function between protein-covered and exposed gold stripes for the three studied cases were compared (Figure 5d) and correlated well with the trend observed for the effects of the proteins on the CPD in the large-scale measurements (Figure 4). In all cases,

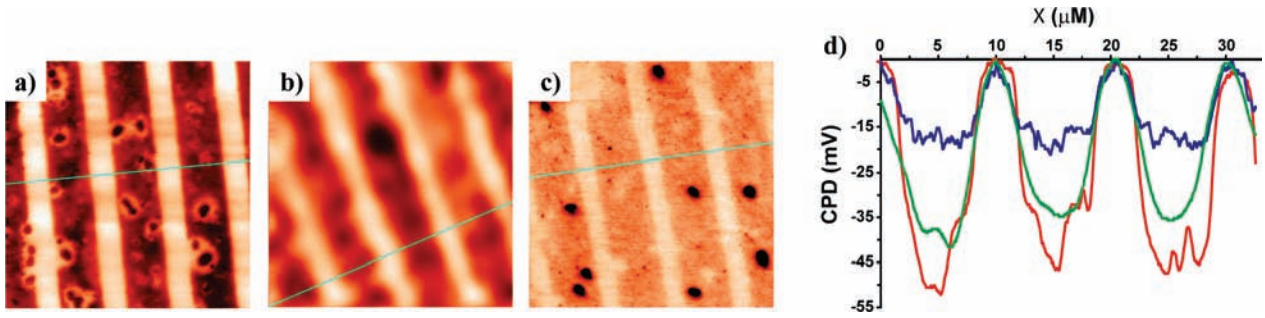

Figure 5. Lateral control of gold surface work function obtained by μCP of coiled-coil proteins. 40 × 40 μm^2 CPD images of patterns of **PC** (panel a), **AP** (b), and **PN** (c) on gold obtained by Kelvin probe force microscopy (z scale = 80 mV). The bright regions of the pattern, which are the bare gold areas (confirmed by the corresponding topography images), were calibrated to zero. The patterns were prepared by pressing (10 s) against the surface a PDMS stamp (prepared from 10 μm period; 5 μm pitch stripe mold) on which the coiled-coil structures were deposited. Line scans along the lines depicted on the images in green are shown in (d) and confirm qualitatively the same trend in work function differences between bare and protein-covered gold as observed in large area CPD measurements (Figure 4).

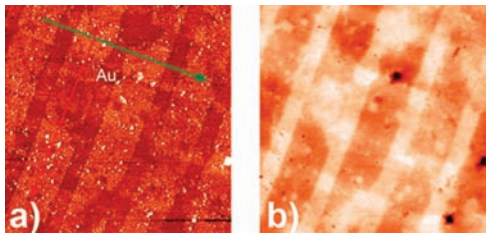

Figure 6. Characterization of molecular net formed by sequential patterning of **PC** and **AP** proteins on gold. Topography (a) and CPD (b) images of samples obtained by perpendicular μCP process of stripes, using the preformed **PC** and **AP** as inks in the first and second layer, respectively. The directions of **PC** and **AP** line patterns are marked by red and green arrows, respectively. The tail of both arrows is placed on a square area on which both proteins were printed. The rectangles separating such mixed areas are covered with **AP**, along the green arrow direction, and **PC**, along the red arrow direction. The lower topography regions (one such square is marked in (a) are uncovered bare gold areas. z scales are 12 nm for the topography (a) and 86 mV for the CPD (b).

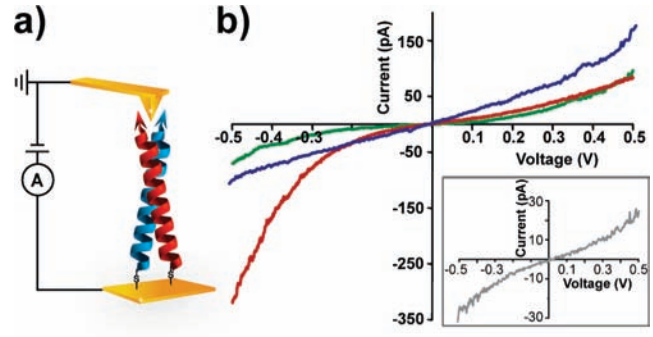

Figure 7. I−V curves of coiled-coil monolayers: (a) schematic illustration of the experimental setup; (b) I−V curves of **PC** (red), **PN** (blue), and **AP** (green). The curves correspond to average current values over tens of measurements, with applied forces of 30−40 nN. Rectification ratios (defined in the text) were found to be 0.27, 1.2 and 1.7 for **PC**, **AP**, and **PN**, respectively. An average I−V curve for **RS** is shown in the inset (R = 1). The overall smaller current obtained for **RS** is due to the smaller forces (less than 10 nN) used in obtaining this data.

lower CPD values were obtained for protein-covered surfaces relative to bare gold, and the (absolute) magnitude of the CPD values was in the order **Pc-Au** > **AP-Au** > **PN-Au**. The smaller work function differences observed in the KPFM measurements can be explained by the formation of less dense and less oriented layers during the μCP process, which can be due to the hydrophobic nature of the PDMS stamp and/or the shorter time used for the assembly process. Overall, these results indicate that the coiled-coil structure is retained through the μCP process with probably only minute unfolding effects.

Further flexibility in surface potential manipulation was achieved by the formation of square patterns via cross patterning of lines made of **PC** and **AP** (Figure 6). Four types of distinctive square and rectangular areas were obtained with different average height (Figure 6a) and CPD (Figure 6b). The highest CPD signals were observed for regions with lower height, corresponding to bare gold. The regions covered with either **PC** or **AP** could be easily distinguished, according to their different CPD signals. Interestingly, in areas covered with both proteins, the CPD values were similar to those obtained for areas covered with only **PC**, probably due to the smaller contribution of **AP** to the CPD.

Coiled Coils with Various Conformations As Molecular Bridges. In previous studies it was suggested that the internal dipole of α-helical peptides induces a rectifying behavior in charge transfer through molecular junctions.[30,37,38] The effects of the protein conformations on electron transport through molecular junctions were studied by recording the current−voltage relations using the gold surface as one electrode, and gold- or platinum-coated AFM tip as a second electrode, and each of the coiled-coil protein monolayers as a molecular bridge (Figure 7). Asymmetric current−voltage relations are observed for both **PC** and **PN**, resulting in rectifying behavior, but with opposite polarity. This behavior results from the proteins' molecular dipole. Since all of the proteins are uniformly oriented between the two electrodes (roughly 50 protein molecules in the junction for each measurement), their overall contribution to the observed current is similar. Thus, for positive potential, for which the external electric field is in the opposite direction to the field of the internal dipole of **PC**, the layer acts as a barrier for electron transfer and a small current is obtained. However, when the external and internal fields are in the same direction (for negative biases) larger currents are obtained with superlinear dependence on the external potential. This is in agreement with the results obtained by Sek at al. for α-helix peptides.[30] The opposite phenomenon takes place for **PN** because of the inversion of the direction of the molecular dipole, resulting in larger current for positive biases. The rectification ratio, defined as $R = |(I(V\text{app} = 0.5\text{V}))/(I(V\text{app} = -0.5\text{V}))|$, was found to be 0.27 and 1.7 for **PC** and **PN**, respectively, in the range of rectification values obtained with similar systems.[30,37,38] Overall, the rectification is smaller than expected from the molecular dipole magnitude, probably due to depolarization effects in the

monolayer as also observed by the CPD results (Figure 4). Interestingly, the rectification is larger for **PC**, due possibly to additional asymmetry originating in the characteristics of the contacts, where a S−Au chemical bond is formed at the surface, while a physical bond is formed at the tip. Studies of the system in Au−S-coiled coil−S−Au configuration are currently being attempted in order to shed light on the role of contact type in determining the current behavior. The effects of protein conformation on electron transfer is reflected by the more symmetric behavior observed for **AP** ($R = 1.2$) that possesses a much smaller dipole. In this case, for both external potential polarities electrons are exposed to about the same internal electric field leading to a similar electron-transfer rate. The symmetric I−V behavior found for **RS** (inset to Figure 7, $R = 1$) further illustrates the role of the protein internal dipole in determining the rectification behavior. Similar conductivity experiments with all proteins were carried out in an air-free, dry, glovebox and resulted in similar behavior suggesting that humidity does not affect significantly the results. As mentioned above, the observed current through the dense monolayers used in our studies is probably a summation of the transport through several tens of molecules in parallel, since each of the molecules holds the same orientation with respect to the surface. Furthermore, since the density of the monolayers is similar, the same averaged amount of molecules is being summed in each of the samples.

The charge transport behavior observed in these studies may be different from that observed previously for α-helical peptides bridges. While in our system the current characteristics are dominated by electron transfer through the protein molecule, in other cases it was observed to be dominated by the protein/electrode interface, leading to an opposite rectification behavior.[38] This may be due to the shorter helix lengths used in those studies. In addition, different conduction mechanisms through the peptides are expected since for short peptides superexchange mechanisms dominate charge transfer, while for longer peptides long-range hoping mechanisms are involved. Furthermore, the conduction mechanism in our system is more complex, as there are at list two different channels of electron transfer through the two different helices comprising the coiled coil.

Conclusions

We have introduced the use of artificial coiled-coil proteins with variable conformations as components of molecular electronic devices. The proteins were assembled with predefined physical orientation and stabilized in a parallel or antiparallel supersecondary structure. Once bound to the surface, their molecular dipole modulated the work function of gold electrodes in two incremental steps (of ∼130 mV). Moreover, the protein conformations affected the I−V characteristics of their molecular bridges, producing either rectifying or nonrectifying (ohmic like) behavior, with the orientation of the molecule determining the rectification polarity. The described modular system can provide new insights into unresolved issues in the phenomenon of electron transport through proteins. In addition, the structural versatility embedded in the coil coiled structures, which is the reason for their diverse functionality in nature, offers ample of options for future design of artificial molecular electronic devices with tailor-made properties. For example, the addition of appropriate solvent exposed side chains can be used to get better conductivity. Finally, the ability of coiled-coil proteins, as well as other systems, to undergo major dynamic conformational changes might be used in the future for controlling the molecular junction electronic behavior in situ.

Experimental Methods

Peptide Synthesis and Characterization. Monomeric peptides were prepared by Fmoc-based solid-phase synthesis on a Rink Amide MBHA resin, at 0.1 mmol scale. Amino acids (0.4 mmol) were attached sequentially using 2-(1*H*-benzotriazol-1-yl)-1,1,3,3-tetramethyluronium hexafluorophosphate (HBTU, 0.4 mmol) as coupling reagent and diisopropylethylamine (DIEA, 2 mmol) as base. Typical coupling times varied between 0.5 and 2 h. Cleavage of the peptides from the resin and global deprotection were then performed in a TFA/TIS/H_2O/EDT (95:2.5:1.5:1 ratio) mixture for at least 2 h at room temperature. Most of the TFA was removed by evaporation, and the crude peptide was precipitated with cold diethyl ether and extracted after centrifugation.

The peptides were purified by reversed-phase preparative HPLC (Thermo Spectra Physics) using a C18 column and a linear water/acetonitrile gradient containing 0.1% TFA. The purity of the peptides was checked by analytical HPLC (Dionex 1100), using a C18 column and a linear water/acetonitrile gradient containing 0.1% TFA. Only samples with 95% purity or higher were used for further analysis in solution or on gold surfaces. The molecular weights of the resulted peptides were verified by mass spectrometry, either on MALDI-TOF (reflex IV Bruker Daltonics; α-cyanohydroxycinnamic acid as ionization matrix) or LCMS (ESI, Thermo Surveyor 355). In all cases, masses of the calculated molecular weight ± 2 units were obtained.

Coiled-Coil Formation and Characterization. Stock solutions of the monomeric peptides (500−1000 μM) in phosphate buffer at pH 7.2 were prepared. The dimers were formed by mixing equimolar amounts of the corresponding monomers and diluting with the buffer if necessary. The resulting mixtures (200−500 μM) were stirred in open air for at least 30 min. The expected dimers were obtained in all cases in good yield, as verified by post-separation by HPLC and LCMS analysis (see Figure 2). The product mixtures were used as is for further analysis.

The formation of the supersecondary coiled-coil structure was evidenced from CD measurements (JASCO-815 CD spectrometer). The CD spectra of 200−500 μM solutions of the preformed complexes were recorded at room temperature in phosphate buffer at pH 7.2 and 100 mM KCl. Data presented is the average of three scans collected with 0.1 nm intervals from 250 to 200 nm.

Adsorption on Gold Surfaces. Gold samples were first cleaned in methanol and acetone ultrasonic bath for 20 min. After drying, the samples were placed in an ozonator (PCD-UVT, Novascan, USA) for 30 min and immersed in EtOH (HPLC grade) for 20 min for removal of oxide layer. The clean samples were then immersed in 500 μM solutions of the preformed dimeric proteins in phosphate buffer at pH 7.2 overnight. The samples were rinsed to remove excess of proteins by dipping three times in water (TDW) and then drying under nitrogen flow.

Surface coverage due to protein adsorption was estimated by the removal the protein layers by immersing the protein-covered gold slides in aqueous solution of the small-molecule thiol β-mercapto ethanol overnight. The excess of β-mercapto ethanol was removed by washing the aqueous solution with diethyl ether, and the water was evaporated to dryness. The leftover coiled-coil proteins were redissolved in a known amount of water (typically 50 μL) and injected to the HPLC. Quantitative analysis of the amount of monomeric proteins was done using a relevant calibration curve. The total amounts of protein molecules and the area of gold surfaces were used to calculate the area per molecule in A^2. Repeating the experiments allowed us to calculate the experimental errors of this method to be up to ±20%.

Layer thickness was monitored by ellipsometry (SE800, Sentech Instruments GmbH, Germany) using 1.46 for the refraction index. The incident light was produced by a xenon arc lamp (XBO) .The spectral range was between 400 and 820 nm, with a spectral

resolution of about 0.6 nm (nearly 700 Del/Psi pairs in each measurement). The incident angle of the light was set at 70°. The values given for each monolayer reflect an average of four different samples, with at least three measurements on each sample. Surface roughness was neglected. Additional thickness measurements were obtained by "shaving" experiments using AFM (Solver Pro, NT-MDT, Ru). In these experiments, local removal of the monolayers was obtained by scanning an AFM tip over the surface applying a large force (tens of nN). A larger area was then scanned with a minimal force in tapping mode, and the thickness of the monolayers was directly obtained by averaging differences in heights between the "shaved" and "unshaved" areas. Control experiments on bare gold samples indicated that this procedure does not remove gold atoms from the surface.

Adsorption on Gold Colloids. Solutions of 330 μM preformed coiled-coil proteins in phosphate buffer at pH 7.2 were prepared, mixed with a suspension of ~0.2 μM gold colloids (custom-made, average diameter 5 nm), and gently stirred at 4 °C overnight. The unbound protein molecules were removed, and the protein-coated colloids were isolated by three cycles of washing, centrifugation, and solvent decantation. Characterization of the secondary structure of the adsorbed proteins was done by recording the CD spectra of the protein coated colloids at room temperature. The CD spectra presented is the average of three independent scans collected with 0.1 nm intervals from 250 to 200 nm. The CD of the last wash supernatant indicated no presence of proteins in the solution.

Protein Patterning by Microcontact Printing. PDMS stamps prepared from molds with stripes pattern (5 μm width, 10 μm period) were used. Immediately before stamping, each stamp was treated in an ozonator for 20 min, washed with ethanol, and immersed in a peptide solution for about 10 s, followed by drying under nitrogen flow. Printing was achieved by pressing the stamp onto gold surfaces (cleaned as described above) for about 10 s, followed by rinsing in TDW and drying under nitrogen flow.

CPD Measurements. SAMs of the proteins on gold were prepared as described above. Samples were mounted in a dark, grounded, Faraday cage. CPD values were acquired, after equilibration in the dark for a few minutes, using the Kelvin probe technique (Besocke-Delta-Phi, Julich, DE). Two to four samples were measured for each SAM with five repeated recordings for each sample.

For high-resolution measurements, images of surface potential were acquired in a lift-off mode (Solver Pro, NT-MDT, Ru). Samples were mounted on AFM disks using colloidal silver glue, applied through the edges to the top gold layer in order to ensure electrical contact. Measurements were done using gold-coated silicon tips (NSG01/Au, NT-MDT, Ru). Images were processed by a line-by-line first-order flattening process. The CPD signal was obtained by taking the minus of the obtained surface potential signal. A constant value was reduced from all images so that the bright areas of the sample (bare gold) reflect the zero CPD value.

Molecular Junctions: Current−Voltage Relations. I−V curves were obtained in a two-point configuration on SAMs of the proteins using the AFM apparatus, with gold- or platinum-coated AFM tips (NSG01/Au, NT-MDT, Ru, or Pt coated ElectroCont-G, Budget Sensors, Bulgaria) as one electrode and the gold surface as a second electrode. The use of both Pt and Au as tip coatings resulted in similar results. Prior to the measurements, the surface was scanned in tapping mode to ensure the formation of a smooth monolayer. The AFM was then switched to contact mode and I−V curves were acquired on a predefined matrix of points (100−900 measurement points in each measured matrix) with the tip grounded and the voltage applied to the sample (see the inset to Figure 7). Forces applied during I−V acquisitions were between 30 and 40 nN (smaller forces of about 3−10 nN were used for the measurements of the reference molecule **RS**). Measurements were acquired both in air and in a nitrogen-filled glovebox with ~1 ppm of oxygen and water (Mbraun, Stratham, NH). No significant differences were observed. The measurements in each matrix were screened to remove curves in which no current was observed for the entire voltage range, highly noisy measurements, or measurements that showed significantly abnormal behavior. The remaining measurements were then averaged.

Acknowledgment. This research was supported by grants from the Israel Science Foundation (G.A., ISF 1291/08; N.A., 1293/08). G.A. acknowledges Career Development Awards from HFSP. We are also grateful for generous support from the Edmond J. Safra Foundation. We thank Moran Amit for help with the preparation of AFM images.

JA907902H